Steady state slow shock inside the Earth's magnetosheath: To be or not to be? 1. The original observations revisited

Daniel Hubert, Andrey A. Samsonov

Steady state slow shock inside the Earth's magnetosheath: To be or not to be?
1. The original observations revisited

D. Hubert

Laboratoire d'Etude Spatiale et d'Instrumentation Astrophysique (UMR 8109/CNRS), Observatoire de Paris, Meudon, France

A. Samsonov

Department of Earth Physics, Institute of Physics, St. Petersburg State University, St. Petersburg, Russia

Received 25 April 2003; revised 20 October 2003; accepted 27 October 2003; published 28 January 2004.

[1] The original data that led to the slow mode transition (SMT) scenario for the diversion of the solar wind flow, in front of the dayside magnetoseath, are reexamined. It is shown that a number of SMT cases on the original list should be rejected because the corresponding solar wind data observed upstream from the magnetosheath display numerous density data gaps or have low time resolution inconsistent with accurate correlation study, or the SMT occurs between two successive crossings of the magnetopause. Therefore the SMT scenario is not established at a statistical level because of the limited number of well-identified cases. Temporal variations of the interplanetary magnetic field (IMF) are shown to play a crucial role in the origin, duration and magnetic field topology of SMTs through the introduction of multiple time shifts in any correlations of magnetic field data obtained on two spacecraft whose distance in a plane perpendicular to the Sun-Earth line is more than a few of tens Earth radius. These temporal IMF variations, correlated with solar wind density enhancements, induce a compressed magnetopause during SMT observations. The exogeneous nature of SMTs is established. Case studies reveal the different processes at the origin of the large enhancement of the density in SMTs with respect to the density upstream of the SMTs. These processes include: (1) an increase of the solar wind density, (2) variations in the density in the magnetosheath linked to increases of the Alfvén Mach number and to a new orientation of the IMF, and (3) a density gradient effect induced in the magnetosheath depletion layer by motion of the magnetopause. Other cases display proeminent density peaks linked to interplanetary magnetic field discontinuities imbedded in the SMTs. We also show that a previous analysis about stationarity of a SMT's front as well as of identification of slow modes propagating against the flow are not confirmed. The exogeneous scenario based on IMF and solar wind density variations for the origin and nature of the SMT phenomenon answers all the questions so far asked about this process. *INDEX TERMS:* 2728 Magnetospheric Physics: Magnetosheath; 2784 Magnetospheric Physics: Solar wind/magnetosphere interactions; 7811 Space Plasma Physics: Discontinuities; 2753 Magnetospheric Physics: Numerical modeling; *KEYWORDS:* magnetosheath, discontinuity, transition, convection, diversion, MHD

Citation: Hubert, D., and A. Samsonov (2004), Steady state slow shock inside the Earth's magnetosheath: To be or not to be? 1. The original observations revisited, *J. Geophys. Res.*, *109*, A01217, doi:10.1029/2003JA010008.

1. Introduction

[2] In the early sixties, a distinct region between the Earth's bow shock and the magnetopause was identified from IMP 1 observations by *Ness et al.* [1964]. This region, called the magnetosheath, was predicted from a fluid model by *Spreiter and Jones* [1963]. The shock not only slows down the solar wind but also affects the particle density and temperature anisotropy, the interplanetary magnetic field modulus and direction. The large scale flow in the magnetosheath was first calculated by *Spreiter et al.* [1966], who derived a stationary solution from the hydrodynamic equations and predicted an increase of the density from the subsolar bow shock to the subsolar magnetopause. However, calculations including the interplanetary magnetic field (IMF), [*Lees*, 1964; *Zwan*

0148-0227/04/2003JA010008

and Wolf, 1976] predict that the magnetic field increases monotonically from the subsolar bow shock to the magnetopause and the density should display a depletion layer adjacent to the magnetopause. This feature was observed for the first time by *Paschmann et al.* [1978] then by *Crooker et al.* [1979]. During the last decade a new picture of the magnetosheath has been developed which includes transient pressure pulses which should play a key role in the unsteady solar wind-magnetosphere-ionosphere coupling [*Sibeck*, 1994; *Sibeck and Gosling*, 1996]. The study of the stationary properties of the solar wind flow and IMF along radial crossings of the magnetosheath by a spacecraft is difficult because of the many variations of the solar wind pressure and of the IMF direction during the crossing [*Fairfield*, 1976], and the result in variations of the magnetopause position and shape [*Sibeck et al.*, 1991; *Shue et al.*, 1997].

[3] A region defined as a slow mode transition region (SMT) in which the density increases while the modulus of the IMF decreases, was identified by *Song et al.* [1990, 1992a]. This phenomenon was observed in more than half of the crossings of the dayside magnetosheath by ISEE-1-2 during the period in 1977–1978. SMTs are statistically defined as stationary structures of about 0.4 R_E thick, standing in the flow 0.2 R_E away from the magnetopause. In these structures, the average density increases about 40%, while the average modulus of the magnetic field is anticorrelated to the density. A relevant question examined by *Song et al.* [1990, 1992a], *Zhang et al.* [1996], *Song and Russell* [2002] was whether the density enhancement in the SMTs is temporal or spatial. They concluded that it is spatial and inherent in a stationary flow in the inner dayside magnetosheath. Indeed, it was found that: (1) the density enhancements occur preferentially in the inner magnetosheath and not randomly throughout the magnetosheath, (2) the relative changes of the solar wind density are usually much smaller than the relative density enhancement in the SMT in front of the magnetopause, (3) there was no dependance on the shear between the IMF and the magnetospheric field, (4) in one case the density structure front appears to propagate upstream in the rest frame of the flow [*Song et al.*, 1992a], (5) in SMTs the density and magnetic field fluctuations display high energy wave activity and in one case slow mode waves propagating sunward and quasi-standing in the SMT have been identified and should build up the outer edge of the SMTs [*Song et al.*, 1992b], and (6) the SMT region, which was not predicted by any of the existing models at that time [*Spreiter et al.*, 1966; *Zwan and Wolf*, 1976; *Pudovkin et al.*, 1982] should divert the stationary flow from the Sun-Earth line [*Song et al.*, 1992a]. Another observation of this phenomenon in the Jupiter's magnetosheath has been reported by *Hammond et al.* [1995].

[4] In a scenario inspired by the SMT's observations, *Southwood and Kivelson* [1992] stressed that in magnetohydrodynamics (MHD), except for fortuitous alignment of field and flow in the magnetosheath, the postshock flow speed is bigger to the speed of intermediate and slow modes. As a consequence, there remains the possibility that slow MHD shock appears in the magnetosheath flow. This scenario predicts the form and geometry of the front [*Southwood and Kivelson*, 1995a]. Moreover, *Southwood and Kivelson* [1995b] noted that the formation of the depletion density layer adjacent to the magnetopause requires the presence upstream of a region of enhanced pressure and field rarefaction.

[5] In regards to the endogeneous nature of the SMTs, we note that slow mode propagation waves play a crucial role in the build up of SMT's external front [*Song and Russell*, 1997, 2002; *Southwood and Kivelson*, 1995b]. The question about the existence of propagating slow modes which should be damped in the magnetosheath, is still open [*Southwood and Kivelson*, 1995a], as well as the existence of monochromatic low frequency modes downstream quasi-parallel shocks [*Lacombe and Belmont*, 1995]. The interplanetary magnetic field (IMF) undoubtedly plays a role in controling the structure of the magnetosheath producing different regions connected through streamlines to quasi-parallel or quasi-perpendicular shocks [*Luhman et al.*, 1986]. The 3-D MHD simulations of the magnetosheath flow by, for example, *Farrugia et al.* [1998] and *Samsonov et al.* [2001] predict the density depletion layer adjacent to the magnetopause but do not predict any standing slow mode region in front of the magnetopause. These aspects motivated our interest to the formation of SMTs. Indeed, *Hubert* [2001] revisited the event on 17 September 1978 on ISEE-2 which has been the most studied. He established that the two edges and the variation of the magnetic field modulus of that SMT have an exogeneous origin and result from two IMF discontinuities observed on ISEE-3 at a large distance from the Sun-Earth line. He concluded that there are many effects which contribute to the density enhancement in this SMT; that there is an enhancement of the density in the solar wind; that there is an increase of the Alfvén Mach number and a new IMF orientation, and that the radial gradient in the magnetosheath sweeps the density past the spacecraft when the magnetopause is compressed. Moreover, from the analysis of the original statistical study by *Song et al.* [1990], *Hubert* [2001] established that all SMTs are correlated to IMF variations.

[6] The purpose of this series of two papers is: in Part 1 to reexamine thoroughly the original observations of SMTs and in part 2 (Samsonov and Hubert, Part 2) to reconciled SMT's observations and 3-D MHD theory. Part 2 provides 3-D MHD simulations of typical SMTs driven by temporal variations of the IMF and solar wind plasma parameters, as well as it discusses whether the MHD theory demands the existence of a steady state slow shock in the magnetosheath flow. Indeed, one of the aspects of the original study by *Song et al.* [1990] is the statistical approach from which the general properties of SMTs were established. We need to deepen this aspect by analysis of all cases in terms of accuracy and temporal resolution of the data involved, as well as the location of the observations by ISEE-1-2. This paper also adresses the role of the low frequency waves in the formation of SMTs not previously discussed by *Hubert* [2001]. As slow modes propagating against the flow [*Song et al.*, 1992b] are part of the scenario presented by *Song and Russell 1997*, 2002] and by *Southwood and Kivelson* [1995a], great attention must be devoted to this aspect. The paper is organized as follows. In section 2 we analyze typical cases illustrating different SMT's events. In section 3 we revisit the original statistics by *Song et al.* [1990] and define different classes

Table 1. Interplanetary and Magnetosheath Parameters Related to SMT Observations[a]

YYMMDD	N_{sw}	**B**	ΔT_B	$\Delta B/B$	$\Delta N/N_{sw}$	θ_u	θ_i	ISEE	ΔT	$\Delta N/N_{sh}$	r_{id}	r_{iu}	C_{ij}
77/11/22	G	G											
78/08/17	8	8	35	−6	50	87	87	1	31	70	0.2	0.9	C_{11}
78/09/27	3	3	30	40	45	150	150	1	34	52	0.2	0.6	C_{11}
78/11/01	3	3	4	−16	15	75	75	1	4	60	0.0	0.1	C_{21}
78/11/06	G	G											
78/11/20	G	G											
77/11/08	G	G											
77/11/12	8	8	11	−15	0			2	11	110			C_{12}
77/11/17	G	8											
77/12/02	G	G											
78/08/10	8	8	11	0	0	95	60	2	10	20	0.2	0.2	C_{11}
78/08/22	3	3	18	−10	0	80	135	1	15	23	0.7	0.3	$C_{11} - C_{21}$
78/09/08	3	3	7	−4	25			2					
78/09/17	3	3	27	−12	10	85	140	1	36	29	0.2	0.4	C_{11}
78/09/21	G	3											
78/09/22	G/3	8/3	7/	−50/0	G/0			2	4	20			C_{12}
78/10/06	8/3	8/3	25/25	−10/0	0/8	137	152	2	25	13	0.3	0.2	C_{11}
78/09/05	G/3	8/3	/	−10/0	G/0	130/	25/	2	30				$C_{11} - C_{21}$

[a] N_{sw}, Reliable solar wind density on IMP-8 or (and) on ISEE-3 is indicated by 8 or 3 (8/3) respectively, many data gaps or too low time resolution data are indicated by G; **B**, Same as N_{sw} but for the IMF; ΔT_B, Interval in minutes of the B field variations; $\Delta B/B$, Relative variation of the modulus |B| in percent, $\Delta B = B_i - B$, B_i is the average of |B| during ΔT_B, B is averaged on 10 min after ΔT_B; $\Delta N/N_{sw}$, Same as $\Delta B/B$ but for the solar wind density; θ_u, Subsolar cone angle defined upstream from the SMT; θ_i, Subsolar cone angle defined during the SMT period; ΔT, Duration in minutes of the SMTs observed on ISEE-1 or on ISEE-2; $\Delta N/N_{sh}$, Same as $\Delta N/N_{sw}$ but for the magnetosheath density; r_{id}, Difference between the subsolar magnetopause distances in Earth's radius at times corresponding to downstream of the SMT and during the SMT, $r_{id} = r_d - r_i$; r_{iu}, same as r_{id} but corresponding to upstream of the SMT and during the SMT, $r_{iu} = r_u - r_i$; C_{ij}, Class of the IMF variation defined above.

of SMTs. Section 4 is devoted to a discussion of our results with respect to the original observations as well as to other observations. Section 5 concludes this first part of the study.

2. Analysis of Cases

[7] We select four typical cases which display complementary SMT's characteristics.

2.1. Case 1 (Day 1978/09/17)

[8] The solar wind density at a time resolution of 24 s [*Bame et al.*, 1978a] and IMF data at 0.167 s [*Frandsen et al.*, 1978] from ISEE-3 were obtained close to the L1 Lagrangian point but at a large distance from the Sun-Earth line. The magnetosheath density was obtained from the electron spectrometer experiment on ISEE-1 at a time resolution of 12 s [*Ogilvie et al.*, 1978], and the magnetic field from the ISEE-1 magnetometer at 0.25 s [*Russell*, 1978]. We choose to use the ISEE-1 density data because in *Song et al.* [1990], the ISEE-2 data in their Table 1 and in their Figure 4, display some inconsistency. Indeed in *Song et al.* [1990] the average density between 1534 and 1610 UT is 15 cm^{-3} in their Table 1 but it is more than 20 cm^{-3} in their Figure 4. Indeed in Table 1, the average density between 1534 and 1610 UT is 15 cm^{-3} but it is more than 20 cm^{-3} in *Song et al.* [1990, Figure 4]. Then, as long as possible we use the ISEE-1 density for any other cases as illustrated further. The five upper panels in Figure 1 display the ISEE-3 data between 1421 and 1611 UT. The 5 lower panels show the corresponding profiles shifted by 54 min, and observed in the subsolar magnetosheath along an outbound crossing. The period between 1534 and 1610 UT in the lower panels was identified as a SMT because it displays an average density 32% larger than the average density measured after 1610 UT [*Song et al.*, 1990], while the corresponding density enhancement in the solar wind between 1440 and 1507 UT is only 10%. Another aspect of the magnetosheath density profile is a density enhancement period of 36 min in the SMT, while the corresponding density enhancement in the solar wind is only 27 min [*Song et al.*, 1992a].

[9] In Figure 1, the top panels show the solar wind density N, the modulus $|\mathbf{B}|$ and the components of the IMF in GSE coordinates. In these panels we note a small enhancement of N anticorrelated to $|\mathbf{B}|$ between 1440 and 1507 UT. The density increase is 10% while the decrease of $|\mathbf{B}|$ is 12% on average with respect to the average values evaluated during 10 min after 1507 UT. This period of time is between two discontinuities: at 1440 UT a discontinuity shows gradual variations of the B_x, B_z components and a sudden variation of B_y. From minimum variance analysis [*Sonnerup and Cahill*, 1967] we determine the normal of the discontinuities taking into account the cutoff criteria defined by *Neugebauer et al.* [1984]. The normal of the discontinuity observed at 1440 UT is $\mathbf{n}_1 = (-0.57, -0.40, 0.72)$ in GSE; the properties of this discontinuity are not typical of a rotational discontinuity in the solar wind [*Hubert*, 2001]. The second discontinuity shows important variations of B_x and B_z at 1507 UT, and the normal is $\mathbf{n}_2 = (-0.60, 0.51, 0.61)$ in GSE. We identify it to be very likely a tangential discontinuity with very small IMF normal components on both sides and an important variation of the IMF modulus across the discontinuity. We observe another discontinuity at 1601 UT characterized by no variation of the magnetic field modulus, that we identify as a rotational discontinuity for which the normal $\mathbf{n}_3 = (-0.43, -0.90, 0.08)$ in GSE is not well defined. The lower panels show the corresponding profiles observed in the subsolar magnetosheath between 1515 and 1705 UT. The magnetopause encountered at 1524 UT displays a clear density overshoot indicated by an arrow in the relevant ISEE-1 density panel. In the SMT, the average density is 29% larger than the average density between 1610 and 1620 UT. The last 12 min of the SMT displays a large

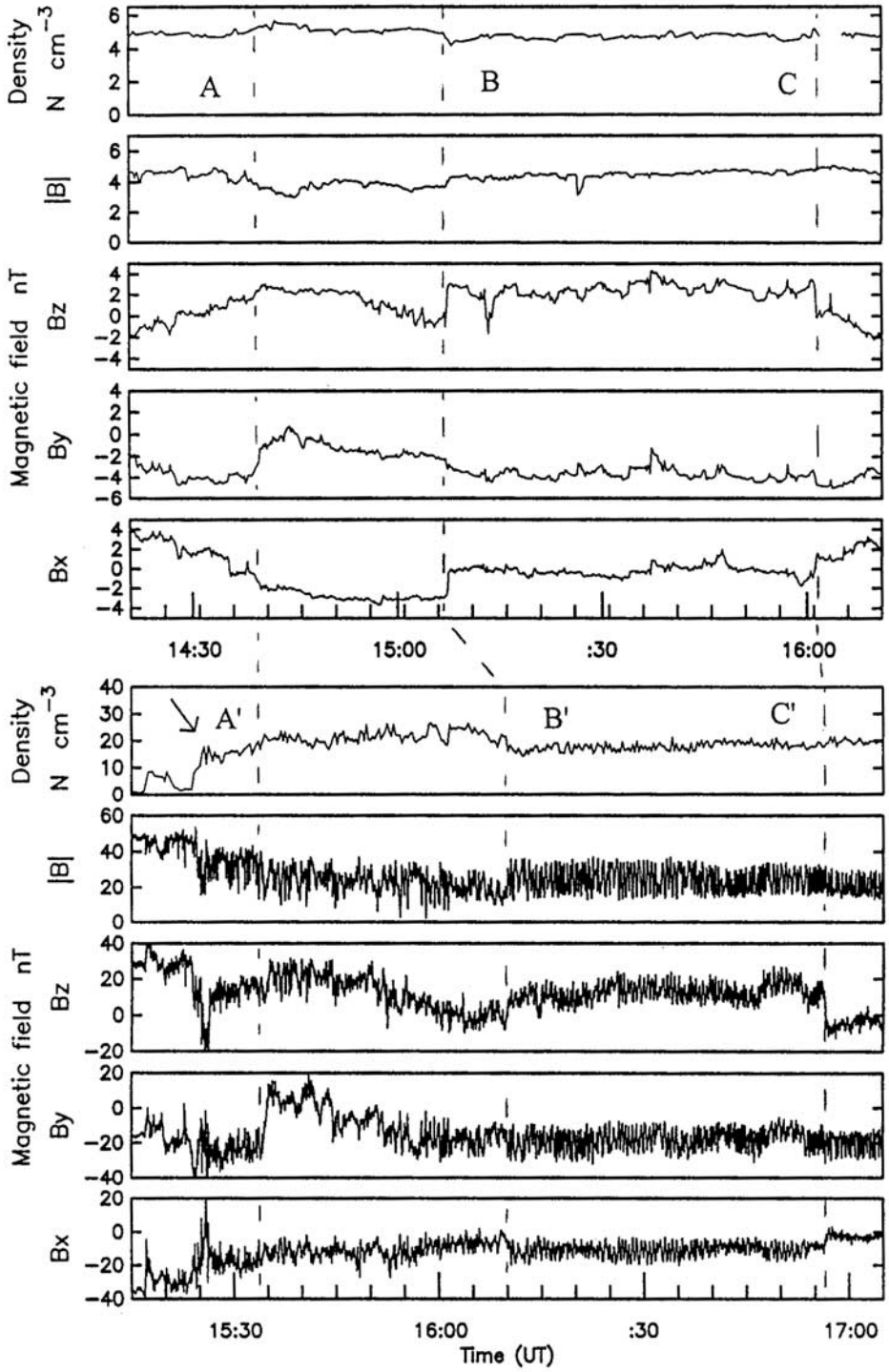

Figure 1. The 5 upper panels show the electron density, the modulus and the GSE components of the magnetic field measured on board ISEE-3, 54 min before the similar measurements made in the magnetosheath on ISEE-2 and represented in the 5 bottom panels.

density enhancement whose average value between 1558 and 1610 UT is 36% larger than the average density between 1610 and 1620 UT. Let us note also that the modulus of the magnetic field in the SMT is 20% lower than the average value between 1610 and 1620 UT. The measurements from ISEE-3 are shifted by 54 min to line up the magnetic discontinuity observed by ISEE-3 at 1440 UT to the field changes observed in the magnetosheath by ISEE-1 at 1534 UT in a similar way as of *Song et al.* [1992a, Figure 5]. These temporal features are linked in Figure 1 by the vertical dashed line AA'. However, in order to explain the magnetic features observed at 1610 UT in the magnetosheath by the temporal variations in the IMF parameters observed in the discontinuity at 1507 UT, we

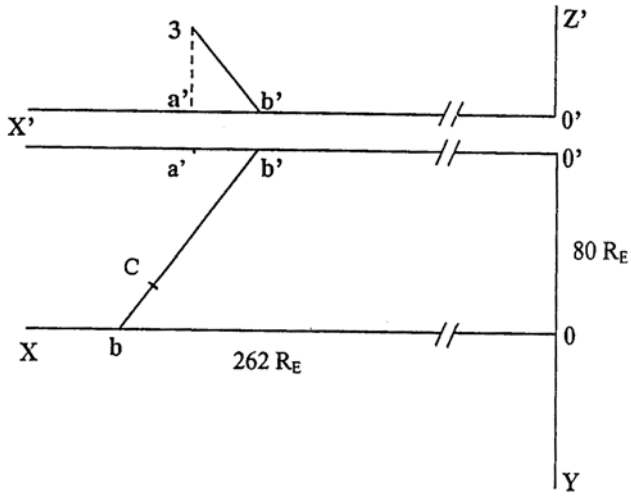

Figure 2. Orientation in a GSE coordinate system of the plane of the tangential discontinuity observed on ISEE-3 at 1507 UT.

must consider a shift of 63 min of the ISEE-3 measurements linking the B and B' events as shown in Figure 1. We note that a timeshift of 55 min connects the IMF discontinuity observed at 1601 to the discontinuity observed at 1656 UT in the ISEE-1 magnetic field as shown by the line CC′ in the Figure 1. Therefore the features AA′ and CC′ have nearly similar timeshifts.

[10] The first important point in this case is to show how the two timeshifts of 54 and 63 min linking AA′ and BB′ respectively can be reconciled. To do so we briefly comment on the demonstration made by *Hubert* [2001]. During these observations, ISEE-3 was at (211, −80, 17) R_E GSE, which is at a large distance from the Sun-Earth line, while ISEE-1 moved from (9.6, −2.25, 4.3) R_E to (10.1, −2.1, 4.5) R_E GSE during the SMT's period of observation. This indicates that ISEE-3 and ISEE-1, which had very different y and z GSE components, were not connected by the same streamline because the solar wind velocity is mainly radially oriented. Let us consider the composite Figure 2; the lower part displays the ecliptic plane XOY with the Earth in O at the origin of the GSE coordinate system, while the O'X' axis is parallel to OX through the projection a' of ISEE-3 in the ecliptic plane, with OO' = −80 R_E; the upper part of this figure shows the X'O'Z' plane in which the Z' coordinate of ISEE-3 is a'3 = 17 R_E with O'a' = 211 R_E. The plane of the tangential discontinuity (TD) is well defined by its normal direction $\mathbf{n}_2$ with an estimated error of 4 degrees. Then, the intersections of the TD plane with the X'O′Z' and XOY planes are respectively the segments 3 b′ with O'b' = 194 R_E and bb' with Ob = 262 R_E at 1507 UT [*Hubert*, 2001]. This shows an unusual orientation of the tangential discontinuity observed at 1507 UT, the plane of which does not tend along the spiral direction as sometimes observed by *Burlaga and Ness* [1969]. Taking into account the aberration of the solar wind flow direction defined by $\varphi = \tan^{-1}(\mathbf{V}_E/\mathbf{V}_{sw})$ where $\mathbf{V}_E$ = (30 km/s) is the Earth's orbital velocity, $\mathbf{V}_{sw}$ the solar wind velocity, the point C along bb' represents at 1507 UT the tangential discontinuity which is observed by ISEE-1 at 1610 UT. The convection time of the TD from C to ISEE-1 is defined from the convection time from C to the bow shock, to which we add the convection time in the magnetosheath to ISEE-1. We obtain 61 min 50 s from the solar wind velocity of 415 km/s measured before 1507 UT and 63 min from the velocity of 405 km/s measured after 1507 UT. These values are very close to the convection time of 63 min linking B to B' in Figure 1. From the direction of the IMF and the ISEE-1 location we deduce that the SMT is observed downstream of a quasi-parallel shock of some 40°, while the upstream region to the SMT was downstream of a quasi-perpendicular shock of some 85°.

[11] The normals of the discontinuities observed by ISEE-3 at 1440 and at 1601 UT are defined with large uncertainty angles, therefore the calculated convection times of these two discontinuities from ISEE-3 to the magnetosheath are not accurate. Nevertheless, we note that the planes of these two discontinuities tend to lie along the spiral direction of the IMF [*Siscoe et al.*, 1968], indicating a smaller convection time from ISEE-3 to ISEE-1 than the convection time of the discontinuity observed at 1507 UT.

[12] A second important point is the analysis of the properties of the discontinuity observed in the magnetosheath at 1610 UT on ISEE-1. This discontinuity is the result of the interaction with the bow shock of the discontinuity observed at 1507 UT on ISEE-3 and convected through the magnetosheath. It is a complex structure that *Song et al.* [1992a] identified to be neither a tangential discontinuity nor a contact discontinuity. Using the normal of this discontinuity, the separation between ISEE-1 and ISEE-2 and the upstream velocity in Table 1 in *Song et al.* [1992a], we find that the convection time by the flow of this discontinuity from ISEE-2 to ISEE-1 is 30 s. Then, in order to explain the observed convection time of the discontinuity of about 1 min between ISEE-2 and ISEE-1, the discontinuity must have a proper velocity of only 20 km/s along its normal with respect to the upstreamflow, indicating that the outer edge of the SMT is not a standing wave front. We note that the general result [*Hudson*, 1970] independent of the type of discontinuity, $(\mathbf{v}_1 - \mathbf{v}_1).(\mathbf{B}_1 \times \mathbf{B}_1) = 0$, is not verified on ISEE-2 at 1609 UT with use of the velocity and field values in Table 1 of *Song et al.* [1992a]; this discrepency makes any further analysis of this discontinuity difficult. The normal of the closest surface of the magnetopause to ISEE-1 determined from Sibeck's model [*Sibeck et al.*, 1991] at 1610 UT is n_p = (0.91, −0.17, 0.38) in GSE. We find that the **B** fields upstream and downstream to the discontinuity at 1610 UT are respectively at 88 and 86 degrees from the magnetopause normal, indicating a draping of the **B** field on the magnetopause.

[13] The third important point is the analysis of the low frequency modes in the SMT between 1535 and 1610 UT. In order to identify the modes in the SMT we use the method developed by the Meudon group [*Lacombe and Belmont*, 1995]. We concentrate our study on the range of frequencies 0.006 to 0.028 Hz (P. Song, private communication, 1997), in which propagating slow modes have been observed in the SMT by *Song et al.* [1992b]. Figure 3 displays from the top panel to the lower panel the evolution of 4 identifiers calculated every 60 s on sliding intervals of 120 s between 1525 and 1625 UT. The SMT is bounded by the vertical dashed lines. This analysis shows that the correlation $C_nB_{//}$ between the density and the parallel

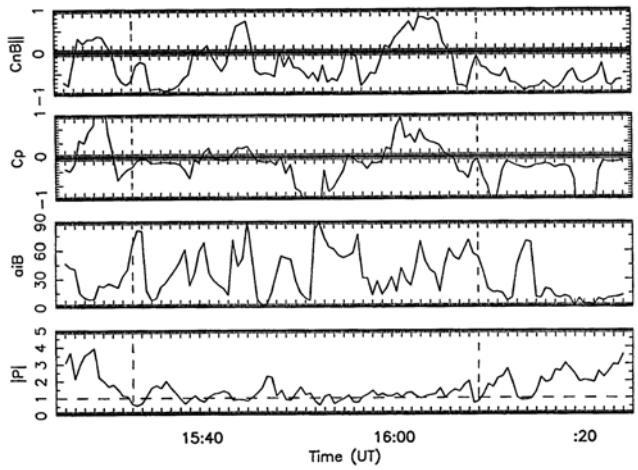

Figure 3. Temporal evolution of the wave parameters of the compressive low frequency modes in the SMT.

magnetic field component, and thus the compressibility C_p which is the real part of the parallel electron compressibility, are highly variable within the SMT. Indeed, they both show major variability with negative and positive values. The maximum variance direction a_{ib} is erratic during the SMT period. The bottom panel displays, for completeness, the magnetic polarization |P| (where |P| is the ratio of the two components of the magnetic field fluctuations, $\delta\mathbf{B}_s$ and $\delta\mathbf{B}_A$; $\delta\mathbf{B}_s$ is in the plane ($\mathbf{k}$, $\mathbf{B}_O$) and $\delta\mathbf{B}_A$ is perpendicular to this plane) which is meaningless as we will show in the next paragraph.

[14] Let us concentrate now on the period of 15 min which extend from 1535 to 1550 UT near the inner edge of the SMT. The variance analysis indicates that the minimum variance direction is defined with a very large error and cannot provide the $\mathbf{k}$ vector direction. The maximum variance direction of the fluctuations on ISEE-1, in the frequency range defined above, is at 41° from the $\mathbf{B}_1$ field direction, and the error made on this direction is 11°. A similar analysis made on the ISEE-2 data shows that the maximum variance direction is at 28° from the mean $\mathbf{B}_2$ field direction, with an error of 20° on the maximum variance direction. The $\mathbf{k}_1$ and $\mathbf{k}_2$ wave vectors defined from the coplanarity theorem, in which the $\mathbf{k}$ vector, the magnetic fluctuations and the average field are in a same plane, ($\mathbf{k}_i = (\delta\mathbf{B}_i \times \mathbf{B}_i) \times \delta\mathbf{B}_i / |(\delta\mathbf{B}_i \times \mathbf{B}_i) \times \delta\mathbf{B}_i|$) are $\mathbf{k}_1$ = (−0.329, −0.801, 0.482) and $\mathbf{k}_2$ = (0.055, −0.842, −0.535) in GSE. While the maximum variance directions $\delta\mathbf{B}_1$ on ISEE-1 and $\delta\mathbf{B}_2$ on ISEE-2 are at 48°, the $\mathbf{k}_1$ and $\mathbf{k}_2$ wave vectors are at 67°, and k_2 is at 13° to the wave vector determined by *Song et al.* [1992a]. We conclude that as the k vector direction is erratic, any propagation time versus convection time cannot be defined with confidence. We obtain similar results when we determine the maximum variance direction and the $\mathbf{k}$ vector during another period of 10 min in the SMT but adjacent to the outer edge.

2.2. Case 2 (Day 1978/08/22)

[15] The solar wind density and IMF are obtained from ISEE-3 cruising toward the L1 Lagrangian point with coordinates (132, −15, 14) R_E in GSE. The magnetosheath magnetic field is provided by ISEE-2 and the density from the Fast Plasma experiment [*Bame et al.*, 1978b] at same time resolution than in case 1. The five upper panels in Figure 4 display the ISEE-3 data between 0811 and 0956 UT while the five lower panels display the corresponding ISEE-2 data in the same order as in Figure 1. A SMT was identified by *Song et al.* [1990] from 0905 to 0920 UT and composed of two prominent density peaks as seen in the relevant ISEE-2 density panel in Figure 4.

[16] The density in the upper panel of Figure 4 displays an increasing trend and many peaks from 0829 to 0846 UT. A density peak, of a few minutes, is noted as '1' in the upper panel and is related to a decrease of the magnetic field modulus observed from 0829 to 0833 UT. This density peak is observed after the vertical dashed line, noted A, which connects the field components of the discontinuity observed at 0829 UT. Then, a new decrease of the magnetic field modulus is observed from 0836 to 0846 UT and two close magnetic discontinuities can be identified around 0842 UT from the B_y component of the IMF. The 5 lower panels show the corresponding measurements by ISEE-2 in the subsolar magnetosheath from 0845 to 1030 UT. The magnetopause was encountered at (10.4, 2.2, 4.4) R_E GSE at 0900 UT. The ISEE-3 measurements are shifted by 34 min to line up the two close magnetic discontinuities observed by ISEE-3 around 0842 UT with the two magnetic field discontinuities observed in the magnetosheath by ISEE-2 at 0916 UT. The B_y components of the two magnetic fields are similar, and the edge of the increase of the ISEE-3 magnetic field, at 0846 UT, corresponds to the outer edge of the increase of the ISEE-2 magnetic field at 0920 UT.

[17] The density structure observed in the ISEE-2 data between 0905 and 0920 UT displays two distinguishable density peaks, noted 1′ and 2′, at about 7 min from each other. They are separated by a period of 3 min in which the density is much lower. Let us consider the IMF discontinuity observed at 0829 UT on ISEE-3 and noted A in the field modulus panel. From a variance analysis, the normal of this discontinuity is defined at 5 degres with $\mathbf{n}$ = (−.61, −.65,0.45) in GSE. Simple calculations of the type we did in section 2.1 show that the plane of this discontinuity intersects the GSE OX axis at 106.7 R_E from the Earth when it reaches ISEE-3. With a solar wind velocity of about 330 km/s, taking into account the aberration of the solar wind flow direction, we deduce that the convection time from ISEE-3 to ISEE-2 is about 37 min. This explains why the interval between the dashed vertical lines A' and B' in Figure 5 is 3 min smaller than the time interval between the discontinuities A and B.

[18] First this analysis shows that the decrease of the IMF modulus from 0829 to 0846 UT and the B_y component observed by ISEE-3 induce the modulus and the B_y components in the SMT observed by ISEE-2. Second, from the IMF components in the upper panel in Figure 4 and the ISEE-2 position, we deduce that the SMT is downstream of a quasi-parallel shock with a shock angle lower than 45° while in the outer edge region, the ISEE-2 spacecraft is downstream of a quasi-perpendicular shock with a shock angle larger than 60°. From the above analysis, we deduce that the density peak 1′ in the magnetosheath is induced by the density peak 1 in the solar wind, while the density

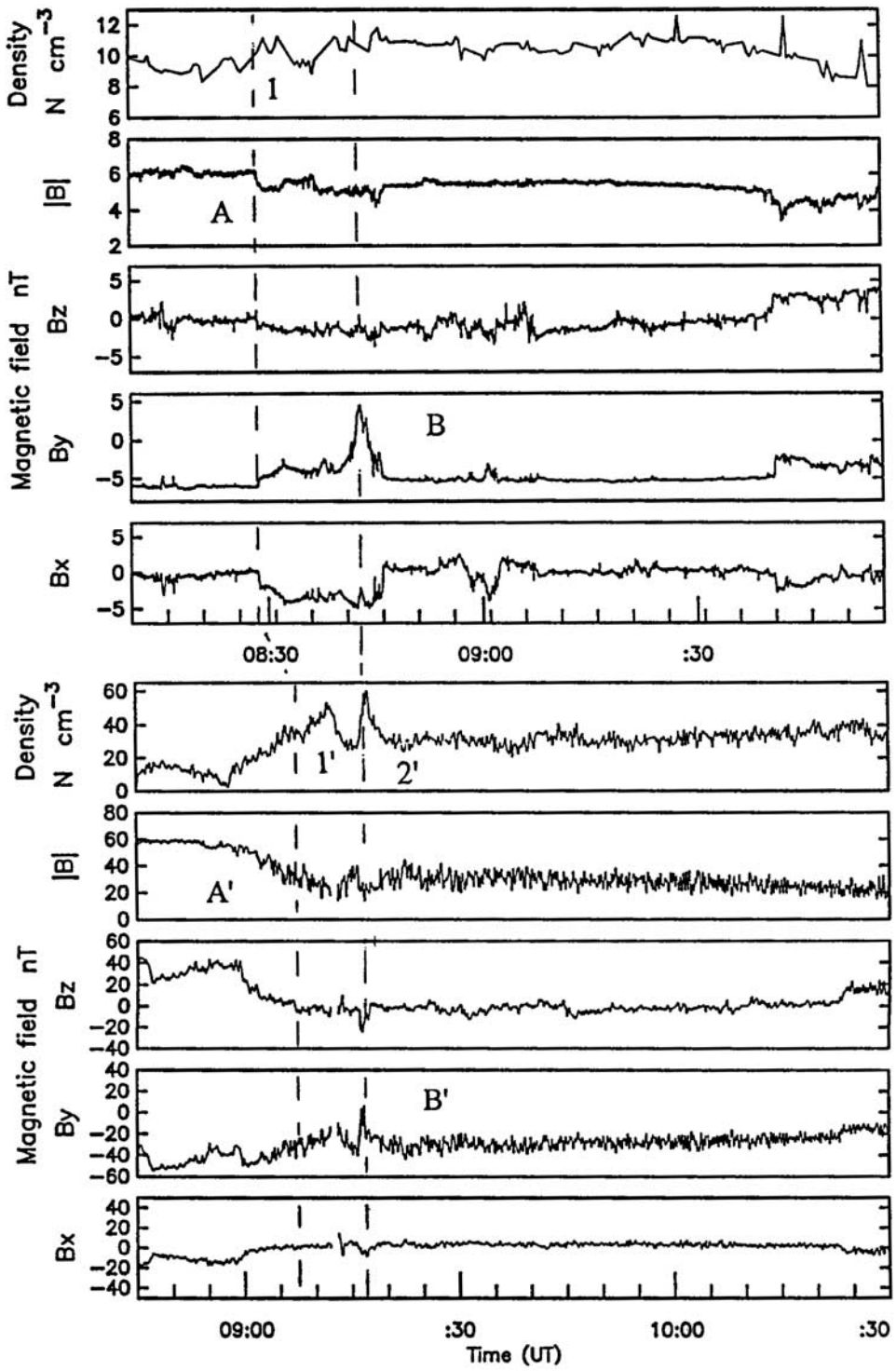

Figure 4. Same presentation as in Figure 1, but for the case 1978/08/22.

peak 2′ is correlated to the IMF discontinuities (denoted B) convected in the magnetosheath.

2.3. Case 3 (Day 1978/09/05)

[19] The 5 upper panels of Figure 5 show ISEE-3 data on September 5, 1978 between 0139 and 0439 UT in the same order as in Figure 1. The five lower panels correspond to ISEE-2 data obtained from an inbound magnetosheath crossing. The timeshift from ISEE-3 to ISEE-2 is about 51 min with ISEE-3 located at (196, −48, 18) R_E GSE, while ISEE-2 was located at (7.6, 9.5, 1.7) R_E GSE at the time of the magnetopause crossing at 0500 UT. A SMT is identified in the ISEE-2 data between 0410 and 0440 UT as indicated by the vertical lines [*Song et al.*, 1992a; *Zhang*

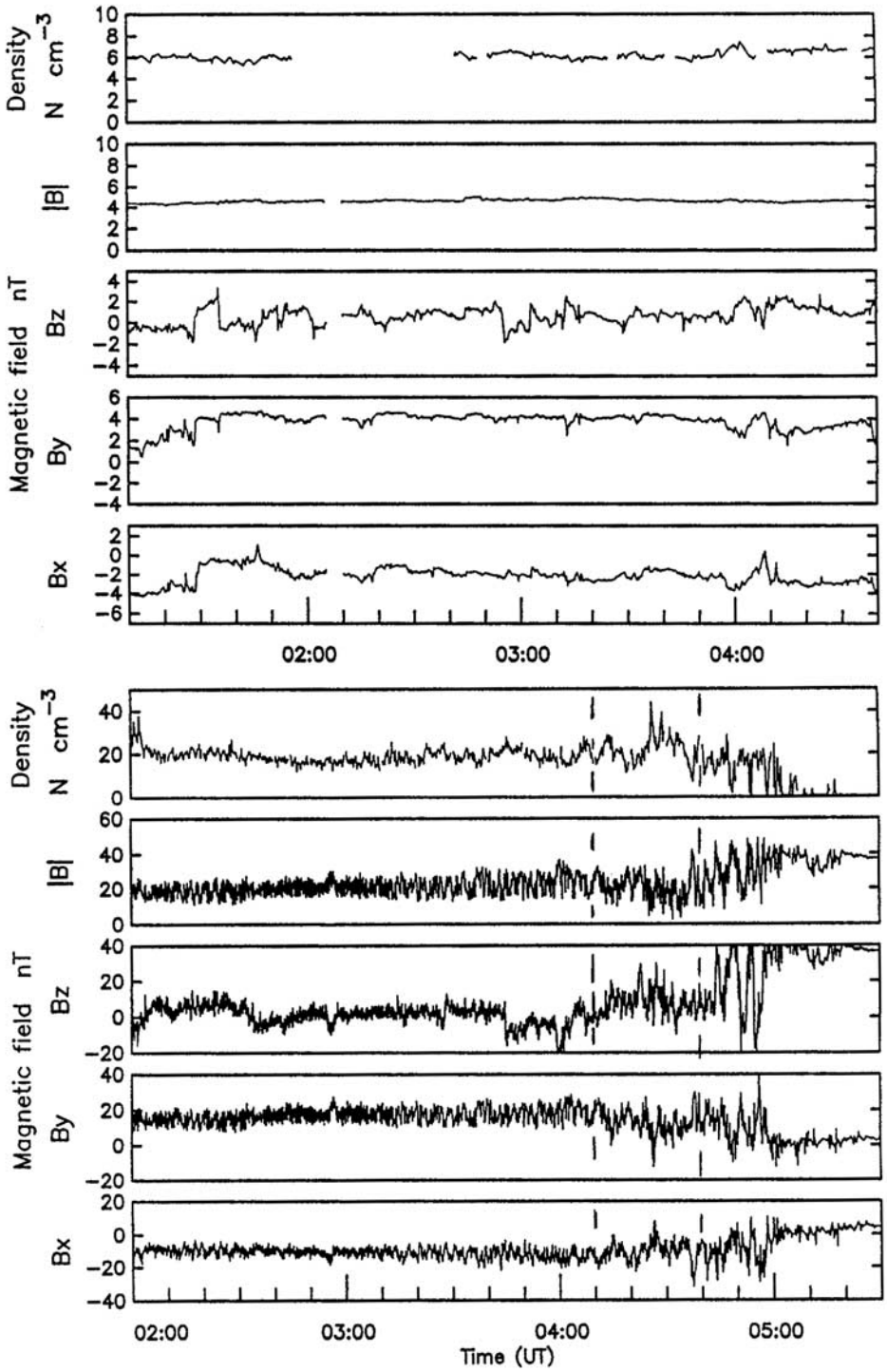

Figure 5. Same presentation as in Figure 1, but for the case 1978/09/05. The five upper panels show ISEE-3 data, the lower panels show ISEE-2 data.

et al., 1996]. The ISEE-3 density and magnetic field did not display any significant variations correlated to the SMT.

[20] Figure 6 presents IMP-8 data for the same day 1978/09/05, when IMP-8 was located at (−6, 33, 4) R_E GSE upstream of the bow shock. The upper panel shows the density at a time resolution of 5 min, and afterward the magnetic field profiles at 15 s between 0200 and 0530 UT while the lower five panels correspond to the ISEE-2 data already presented in Figure 6. There is no density data after 0316 UT. A significant new orientation of the IMF is observed at 0408 UT in the IMP-8 data which is not observed in the ISEE-3 data at an earlier time. In particular, the B_x component evolves from negative values around −3 nT to positive values around 3 nT, while on ISEE-2 the B_x negative component is consistent with a draping field

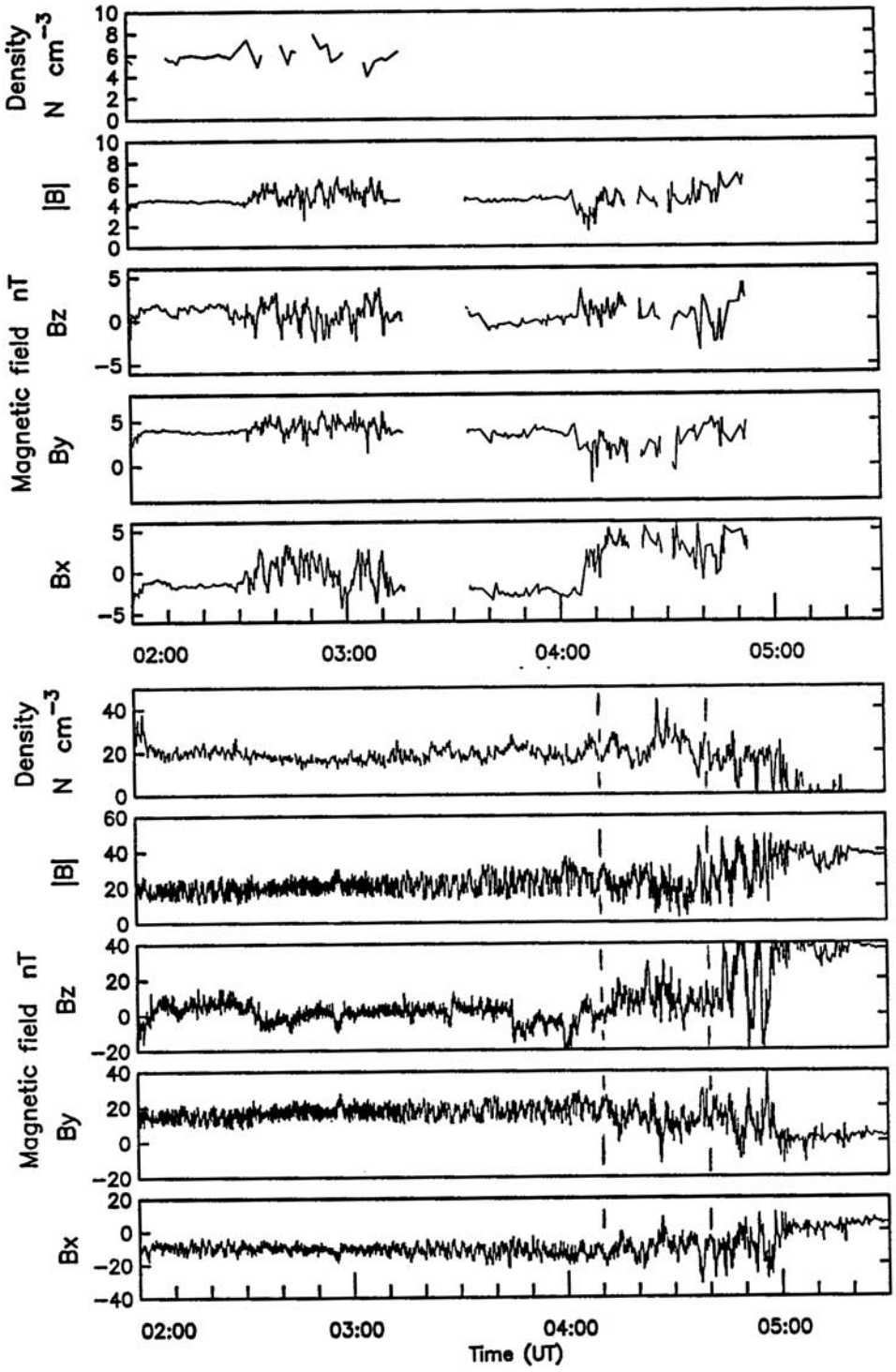

Figure 6. Same presentation as in Figure 5, but the five upper panels show IMP-8 data.

against the magnetopause. The observations on ISEE-2 are made downstream of a quasi-perpendicular shock (shock angle between 60° and 90°) before 0408 UT, that is before the SMT observation, and downstream of a quasi-parallel shock (shock angle lower than 45°) during the SMT's observation when considering the evolution of the IMF direction as well as the position of ISEE-2. The new orientation of the IMF at 0408 UT corresponds nearly to the beginning of the SMT. A data gap of the density from IMP-8 prevents us from analyzing the evolution of this parameter after 0316 UT and correlating it with the SMT density profile.

2.4. Case 4 (Day 1978/09/22)

[21] To discuss this case, it is unnecessary to consider the interplanetary data. The five panels in Figure 7 show

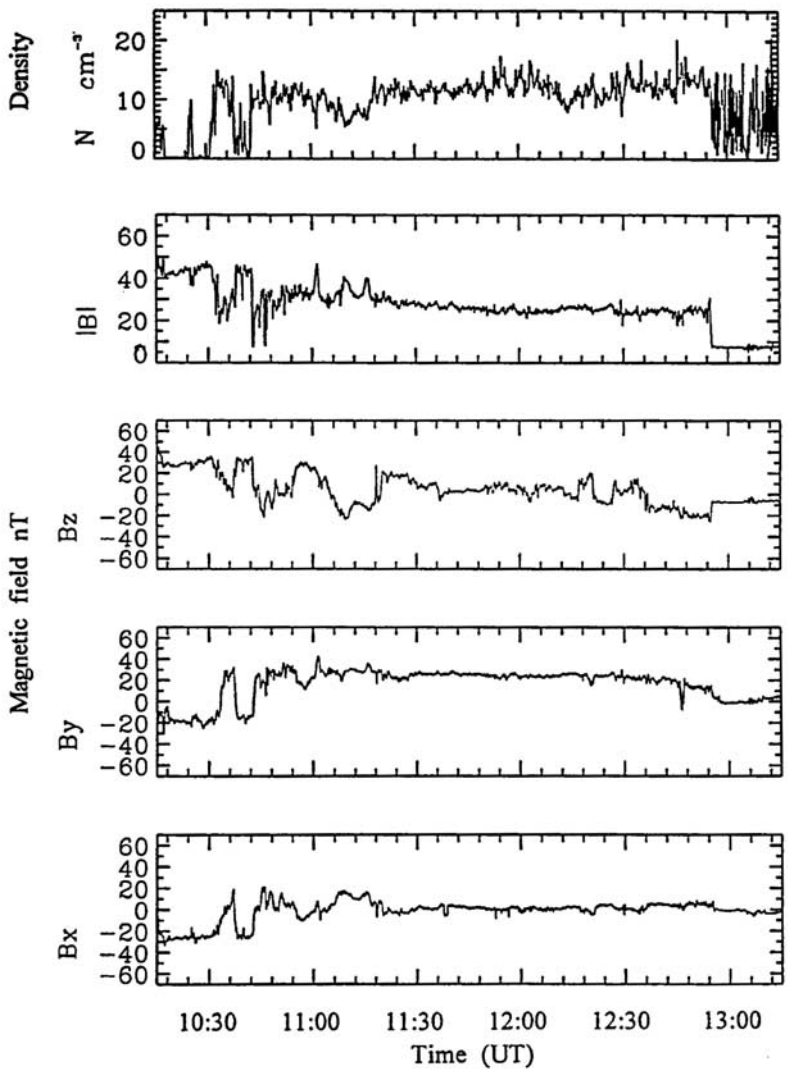

Figure 7. ISEE-2 data for the case 1978/09/22.

data measured by ISEE-2 on 22 September 1978 in the same order as in Figure 1. The measurements are made on ISEE-2 along an outbound crossing of the magnetosheath between 1015 and 1315 UT. The SMT identified by *Song et al.* [1990] begins at 1032 UT with a duration of 4 min. The density, the magnetic field modulus and components profiles show clearly three successive crossings of the magnetopause: the first is at 1032 UT when ISEE-2 enters into the magnetosheath; the second is at 1037 UT when ISEE-2 enter into the magnetosphere; and the third is at 1042 UT with a new entry into the magnetosheath. These magnetopause crossings are very likely induced by IMF modulus, B_x and B_y components variations observed in the IMP-8 magnetic field data (not shown) which unfortunately do not display density data because of a data gap. It is interesting to stress that no specific density and magnetic field variations are observed in the corresponding ISEE-3 data which was located near the L1 Lagrangian point. This SMT is sandwiched between two successive crossings of the magnetopause 5 min apart and does not represent a stationary process of the flow in the inner magnetosheath. This case does not need further analysis.

3. Statistics Revisited

[22] The original statistics were established from a study of 26 crossings among which 17 show the SMT's characteristics presented in *Song et al.* [1990, Table 1]. We study another case already presented in section 2.3 (day 78/09/05). We focus our attention on the relationship between the variations of the solar wind density and interplanetary magnetic field variations (IMFV) observed on ISEE-3 or on IMP-8, with the SMT's density and **B** field observed on ISEE-1-2, taking into account the convection time from the solar wind observations to the magnetosheath observations. Our findings are summarized in Table 1. The interplanetary parameters in the left hand side are defined in the legend, while the parameters connected to the observations in the magnetosheath are in the right hand side. The parameters are the variation of the subsolar cone angle θ related to the SMTs, ($\theta = \cos^{-1}(B_x/|B|)$, where B_x is the x component of

the IMF in GSE) and the variation of the subsolar magnetopause position defined from the Shue's model [*Shue et al.*, 1997]. This model considers the solar wind dynamic pressure and the B_z component at different times related to the SMTs. To make the comparison easier with the *Song et al.* [1990, Table 1] study, we have organized our table in the same order with the last event being the added case of day 1978/09/05.

[23] The analysis of the IMFV as well as the density and magnetic field crossing profiles on ISEE-1-2 lead us to define the SMTs in term of classes C_{ij}. In this classification we consider two aspects: the index i is related to the IMFV observed by ISEE-3 or IMP-8 and corresponding to a given SMT, while j is related to the SMT's location in the magnetosheath with respect to the magnetopause crossings observed by ISEE-1-2. C_{1j} represents the events which display two edges defined by two IMF discontinuities separated by an interval ΔT_B, a possible variation of the modulus of **B** between the two discontinuities as well as its direction defined by the subsolar cone angles θ_i and θ_u. θ_i is defined at a time during the IMFV corresponding to the SMT, and θ_u is defined at a time after (before) the SMT observation if the ISEE-1-2 orbit leg is outward (inward). The class C_{2j} is defined by similar characteristics to the C_{1j} class but also contains IMF discontinuities in the interval ΔT_B. The events in class C_{i1} are observed during uninterrupted crossings of the magnetosheath from the bow shock to the magnetopause (or in the opposite direction), while C_{i2} represents a SMT observed between two successive magnetopause crossings. The events analyzed in section 2.1, 2.2 and 2.4 are respectively typical of the classes C_{11}, C_{21} and C_{12}.

[24] From the results presented in Table 1, we note that for seven cases in *Song et al.* [1990, Table 1] study there is no reliable density data at the appropriate time in the free solar wind. Indeed, long time periods of density data gaps or multiple data gaps of a few minutes during the relevant intervals of time are inconsistent with a careful analysis of the origin of the SMTs. The case 78/09/08 is a misidentification of a SMT. Indeed we note that the ISEE-2 density enhancement is observed in the magnetosphere, and that the ISEE-2 density is about 50% of the ISEE-1 density in the magnetosheath. We identify also that the two cases 1977/11/12 and 1978/09/22 (see section 2.4) display SMT observations between two successive crossings of the magnetopause. It is clear that the SMT is being built up by the back and forth motion of ISEE-1-2 into the depletion layer. These two cases in class C_{12} do not display typical steady state density and magnetic profiles along complete crossings of the dayside magnetosheath. Therefore only eight cases in Table 1 are SMTs observed in the magnetosheath between successive bow shock and magnetopause crossings or the reverse and for which reliable solar wind densities and IMF are available.

[25] We describe the reliable SMT cases which have not been discussed in section 2 of this paper in order to present their main characteristics and to select candidates for the numerical simulations presented in the part 2.

3.1. Case 1978/08/17

[26] The ISEE-1 density shows a large enhancement with respect to the density upstream of the SMT. Moreover, a slice of plasma lasting a few minutes with a density as high as 90 cm^{-3} is observed in the core of the SMT. The IMP-8 density displays a large enhancement (see Table 1) corresponding to the SMT period but it is probably underestimated because there is no measurement corresponding to the slice of high density in the magnetosheath. Indeed, the best time density resolution on IMP-8 for this event is only 5 min (J. Richardson, private communication, 2002). This prevent us from considering this case in a numerical simulation. From the position of ISEE-1 as well as the IMF direction, we deduce that this SMT and its upstream region are downstream of a quasi-perpendicular shock.

3.2. Case 1978/09/27

[27] A large enhancement of the density as well as of the IMF modulus is observed at ISEE-3 during the period of time corresponding to this SMT as indicated in Table 1. This SMT and its upstream region are observed downstream of a quasi-parallel shock. This case is simulated in part 2.

3.3. Case 1978/11/01

[28] The density enhancement observed on ISEE-1 is only 4 min. The density as well the IMF observed on ISEE-3 display many variations of a few minutes and two of them, with large densities, correspond to the SMT. Let us stress also that a portion of this SMT could correspond to a magnetopause density overshoot [*Hubert et al.*, 1998] similar to the one indicated by an arrow in the ISEE-1 density in Figure 1. This SMT and its upstream region are downstream of a quasi-perpendicular shock. The low time resolution of the ISEE-3 density prevent us from selecting this case for simulations.

3.4. Case 1978/08/10

[29] Many variations of the density as well as IMF discontinuities are observed on IMP-8 during the period of time corresponding to the SMT. The density observed on ISEE-2 is underestimated with respect to the density on ISEE-1. Unfortunately the observation on ISEE-1 begins after the SMT period because of an important data gap. The upstream region of this SMT is downstream of a quasi-perpendicular shock, while the SMT is downstream of an oblique shock (shock angle between 45° and 60°). The low time resolution of 90 s of the density measured on IMP-8 and the underestimation of the ISEE-2 density, prevent us from simulating that case with enough confidence.

3.5. Case 1978/10/06

[30] The SMT observations are made downstream from a quasi-parallel shock, while the upstream region is observed downstream from an oblique shock. IMP-8 which is located in the quasi-parallel foreshock provides the density with low time resolution and large variations. The density also measured by ISEE-3 displays many data gaps of a few minutes. This case cannot be selected for simulations.

[31] From Table 1, we note that each SMTs is connected to an IMFV which has nearly the same duration ΔT_B as the duration ΔT of the corresponding SMT. Most of the time, the IMFV displays a decrease of the modulus of the magnetic field correlated with an increase in the density. From the subsolar cone angles, θ_u and θ_i, we deduce that SMTs are correlated to important IMF direction variations. Most likely, SMTs are observed downstream of quasi-

parallel shocks, while upstream from the SMTs the magnetosheath observations are downstream of quasi-perpendicular shocks or of oblique shocks. The two upper cases in Table 1 display major solar wind density increase. Another important property shown in Table 1, is that the subsolar magnetopause distance r_i, during a given SMT, is smaller than the subsolar magnetopause distance r_d downstream of the SMT because $r_{id} = r_d - r_i > 0$. Similarly r_i is smaller than the subsolar magnetopause distance r_u upstream of an SMT because $r_{iu} = r_u - r_i > 0$. This indicates that the SMTs are correlated to motions of the magnetopause and are observed during magnetosheath compressions. This analysis shows also many discrepencies between the ISEE-1 and ISEE-2 densities. The ISEE-1 densities are to be preferred to the ISEE-2 densities because they never display inconsistency when compared to the densities predicted by the Rankine-Hugoniot relations across the bow shock.

4. Discussion

[32] Among the list of SMTs identified in *Song et al.* [1990, Table 1] study a number of cases should be eliminated. They are (1) the cases for which there is no density data, or the density data are corrupted by many data gaps in the solar wind data for the corresponding SMTs observed by ISEE-1-2 in the magnetosheath and (2) the SMT cases observed between two successive magnetopause crossings as they do not display the characteristics of a steady magnetosheath flow. Therefore the list in Table 1 should be reduced from 18 SMT's cases to only 8 candidates for the SMT scenario. This limited number of well-identified SMTs, as well as the lack of published results on the enhancements of the density in the outer magnetosheath do not provide any statistical support for the SMT's scenario.

[33] Our analysis reveals that SMTs are most of the time related to significant variations of the IMF, with moderate solar wind density enhancements and downstream quasi-parallel shocks. Other cases display small variations of the IMF but significant enhancements of the solar wind density. From Shue's model [*Shue et al.*, 1997] we deduce that, during the SMTs, the magnetopause is closer to the Earth than before or after the SMTs. These results show that temporal IMFV and solar wind density variations are connected to the origin of the SMT's phenomenon. Moreover, these temporal variations imply that during the SMT observation, the magnetopause is more compressed than before or after these periods of time.

[34] The detailed analysis of the IMFV and solar wind density variations occuring on 17 September 1978, which is the best-documented case, sheds light on the origin of SMTs. As such, the two edges of the IMFV observed with a time interval of 27 min on ISEE-3 at a large distance from the Earth-Sun line are magnetic discontinuities whose planes are not parallel. We have shown how the discontinuities induce the two edges of the SMT observed on ISEE-1-2 with a time interval of 36 min, as ISEE-3 and ISEE-1 where not on the same streamline. This result shows that multitime delays should be used to correlate magnetic field data obtained from different spacecraft at large distance in the YZ GSE plane as also concluded by *Weimer et al.* [2002]. This findings desagree with the method used by *Song et al.* [1999a] which ignores any IMF tilting effect. Furthermore, the decrease of the modulus of the magnetic field in the SMT is a consequence of the decrease of the IMF modulus during the corresponding periods of time. Also, the variations of the B_y and B_z components in the SMT as well as in the adjacent regions are directly explained by the variations of the IMF corresponding components when considering multitime delay; the B_x component does not show much variations because of the draping of the magnetic field on the magnetopause surface. Finally, the spiky nature of the magnetic fluctuations in the SMT is typical of the magnetic and density fluctuations observed downstream of quasi-parallel shocks.

[35] Our analysis about the nature of the low frequency waves in the SMT of 1978/17/09 shows that a **k** vector direction cannot accurately be determined because the maximum variance direction on both spacecrafts is not accurate and is very different. Then the propagation time of the low frequency waves between ISEE-1 and ISEE-2 cannot be accurately determined in order to separate the convection velocity from the propagation velocity of slow MHD modes. Moreover, the parameters of the magnetic fluctuations, from our analysis, are not typical of slow mode waves. This result is in agreement with studies which conclude that the fluctuations dowstream of a quasi-parallel shock should be analysed with turbulence tools.

[36] In the analysis presented by *Song et al.* [1992a, 1992b] it is concluded that the outer edge of the SMT of the day 1978/09/17 is quasi-stationary, being built up by slow mode waves propagating upstream, but we have demonstrated how it is not possible to identify propagating slow modes in this SMT in section 3.1. *Song et al.* [1992a] assumed that the convection time for the solar wind plasma flowing from ISEE-2 to ISEE-1 is the ratio of the separation between the two spacecrafts along the flow divided by the flow velocity; the authors considered this value to be the convection time of the outer edge of the SMT. In our opinion, this approach which leads to the important conclusion that the outer edge is a standing wave front is erroneous because the convection time of the outer edge must be determined from the normal vector direction of this structure. This conclusion leads to a contradiction when considering the normal calculated by *Song et al.* [1992a]. Indeed our calculation shows that the outer edge discontinuity of the SMT has a moderate convection velocity with respect to the flow. Recently *Song and Russell* [2002] stressed that the time shift of the discontinuity observed at 1507 UT on ISEE-3 is controlled by the two discontinuities observed at 1440 UT and 1601 UT on ISEE-3 and observed about 54 min later on ISEE -1; therefore the discontinuity observed on ISEE-3 at 1507 UT should have the same time shift of 54 mn, and we should observe its signature around 1601 UT on ISEE-1 but this is not the case. We have established another coherent picture, with the outer edge of the SMT being the convected discontinuity observed previously on ISEE-3 at 1507 UT but not the stationary front considered by *Song et al.* [1992a] or predicted by the Southwood-Kivelson's scenario [*Southwood and Kivelson*, 1995a].

[37] From the ISEE-1 measurements, the density enhancement in the overall SMT of day 78/09/17 with respect to the average density on a period of 10 min upstream from the outer edge is 29% and it is 36% when considering the period of largest density in the SMT, between 1558 and 1610 UT. The value of 29% is a little different than the

earliest estimation of 32% on ISEE-2 [*Song et al.*, 1990]. The second enhancement that we estimate with a value of 36% is not directly comparable with the value of 50% at 1610 UT defined recently from ISEE-2 data by *Song et al.* [1999b] as we use the ISEE-1 density and as the exact definition of the 50% enhancement is not given in the relevant paper of *Song et al.* [1999b]. We identify different phenomena at the origin of the increase of the density in this SMT. These new findings are: an exogeneous enhancement of 10% of the density in the solar wind during the relevant period; a second effect is related to an increase of the Alfvén Mach number induced by the decrease of the IMF modulus; a third effect, induced by variations of the subsolar cone angle of the IMF, is connected to the properties of the subsolar flow near the magnetopause downstream of a quasi-parallel shock, as compared to the flow downstream of a quasi-perpendicular shock [see *Samsonov and Hubert*, 2004]; and a fourth effect is related to the gradient of the density in the depletion layer and of the motion of the subsolar magnetopause during the time periods of the SMT observations. Indeed, because the magnetosheath is more compressed during the SMT period, the relative position of ISEE-1-2 is in the middle of the magnetosheath where the density is larger than in the depletion layer. When the outer edge of the SMT progresses toward the magnetopause, ISEE-1-2 leave the SMT while the magnetopause distance to the Earth increases; then ISEE-1-2 is closer to the magnetopause and inside the depletion layer, where the density is lower than in the middle of the magnetosheath. Let us stress that in the Spreiter fluid model there is no depletion layer in the subsolar magnetopause. On the contrary, the gradient of the density in that model is opposite to the one in the depletion layer, therefore, the motion of the magnetopause during SMT observations should induce a density decrease in the Spreiter's model.

[38] A balance between the different effects at the origin of the density enhancement of the day 1978/09/17 can also be considered for the other SMTs of the type C_{11}. This is due to the fact that we have always identified corresponding solar wind density increase or IMFV which induce similar density enhancements in the inner magnetosheath. The case 1978/08/22 which is of the type C_{11}–C_{21} has a first density peak explained by the above effects and a second peak correlated to two close IMF rotational discontinuities convected in the magnetosheath after interaction with the bow shock. It has been shown, in numerical 3-D MHD simulations by *Cable and Lin* [1998], how the interaction of an IMF rotational discontinuity with the bow shock provides a density pressure pulse. *Hubert and Harvey* [2000] have observed density pressure pulses from one isolated discontinuity and from two close discontinuities in which the two close density pulses merge together in an extented density enhancement. This peak effect can be extended to the case 1978/08/10 which displays many magnetic field discontinuities. For the 2 cases, 1978/08/17 and 1978/09/27, the density increase in the solar wind is very important and should explain directly the SMT's density enhancement. The case 1978/09/05 is very interesting because a magnetic discontinuity is observed at 0408 UT on IMP-8 that is not identified on ISEE-3, while these two spacecrafts were separated by 41 R_E in the YZ GSE plane. This observation is consistent with *Richardson and Paularena* [2001] results which show that the typical scale length of the IMF is about 45 R_E in the plane perpendicular to the flow. As there is a density data gap on IMP-8 after 0317 UT, we do not confirm the endogeneous origin of this SMT as *Zhang et al.* [1996] concluded. On the contrary, as a smaller modulus of the **B** field is observed on IMP-8 after 0408 UT a corresponding density increase is probably more likely. This effect added to the new orientation of the IMF induces new parameters of the magnetosheath flow.

5. Conclusion

[39] From a revisited analysis of the data at the origin of the SMT phenomenon we conclude that a number of cases should not be retained in the original list. The cases are eliminated because they display data gaps or bad time resolution of the density measurements in the solar wind corresponding to the duration of SMTs observed in the magnetosheath, or they are erroneous identifications due to non-stationary flows in the magnetosheath between two successive magnetopause crossings. Therefore the SMT process is not established at a statistical level because of the limited number of eight cases.

[40] We have established that specific temporal interplanetary magnetic field variations are correlated to the origin of any SMTs. Through the introduction of multiple time shifts for observations near the L1 Lagrangian point, IMF variations determine the edges of the SMTs, that is, their duration, as well as the modulus and magnetic field components in the SMTs. Moreover, these IMF variations are most of the time associated with solar wind density increases. We do not confirm the presence of slow mode waves in the SMT of day 1978/09/17. Contrary to *Song et al.* [1990, 1992a], *Zhang et al.* [1996], we conclude that the origin and nature of the SMT phenomenon is exogeneous rather than endogeneous in origin.

[41] The density enhancements in SMTs is a balance between different process which are identified as follows: (1) part of this density enhancement is due to the solar wind density enhancement related to the IMFV; (2) contributions are related to the control of the profile of the density in the inner magnetosheath by an increase of the Alfvén Mach number through the decrease of the IMF modulus, or by a decrease of the upstream shock angle; (3) another process is related to the density gradient of the magnetosheath depletion layer and its motion with the subsolar magnetopause in response to temporal variations of the interplanetary B field and solar wind dynamic pressure; and (4) density pressure pulses connected to rotational IMF discontinuities convected through the magnetosheath are at the origin of isolated or merged density peaks embedded in SMTs.

[42] This study demonstrates that the temporal flow characteristics of the dayside magnetosheath are strongly correlated with the temporal properties of the IMF and solar wind flow. It shows that a spacecraft monitor close to the Sun-Earth line is required to describe accurately and easily the plasma flow properties in the magnetosheath. Therefore any enhancement of the density observed in the inner dayside magnetosheath, a candidate for an SMT, must be compared to the time variations of the solar wind and IMF observed upstream in the free solar wind. This cannot always be done due to a lack of data as for the examples

on AMPTE and WIND missions in the Earth's magnetosheath, as well as in the Jovian magnetosheath from Ulysses, presented in *Song and Russell* [1997, Figure 5] or in *Song and Russell* [2002, Figure 4].

[43] In conclusion, we have established an exogeneous scenario for the origin and nature of the SMT phenomenon. In the part 2 [*Samsonov and Hubert*, 2004] the existence of the SMTs is addressed in the context of the theoretical background of solar wind flow diversion in the dayside magnetosheath.

[44] **Acknowledgments.** The authors thank the ISEE-1-2-3 and IMP-8 Principal Investigators (J. T. Gosling, A. J. Lazarus, R. P. Lepping, K. W. Ogilvie, C. T. Russell, and E. J. Smith) for providing directly or through the NSSDC, the data for this study. As well we thank J. H. King, J. D. Richardson and P. Song for providing complementary informations. We are grateful to C. Lacombe and G. Atkinson for useful clarifications. We thank the reviewers for their valuable and useful suggestions.

[45] The Editor thanks David Sibeck and another referee for their assistance in evaluating this paper.

References

Bame, S. J., J. R. Asbridge, H. E. Felthauser, J. P. Glore, H. L. Hawk, and J. Chavez (1978a), ISEE-C solar wind plasma experiment, *IEEE Trans. Geosci. Electron.*, *GE-16*, 160.

Bame, S. J., J. R. Asbridge, H. E. Felhauser, J. P. Glore, G. Paschmann, P. Hemmerich, K. L. Ackerson, and H. Rosenbauer (1978b), ISEE-1 and ISEE-2 fast plasma experiment and the ISEE-1 solar wind experiment, *IEEE Trans. Geosci. Electron.*, *GE-16*, 216.

Burlaga, L. F., and N. F. Ness (1969), Tangential discontinuities in the solar wind, *Sol. Phys.*, *9*, 467.

Cable, S., and Y. Lin (1998), Three-dimensional MHD simulations of interplanetary rotational discontinuities impacting the Earth's bow shock and magnetosheath, *J. Geophys. Res.*, *103*, 29,551.

Crooker, N. U., T. E. Eastman, and G. S. Stiles (1979), Observations of plasma depletion in the magnetosheath at the magnetopause, *J. Geophys. Res.*, *84*, 869.

Fairfield, D. H. (1976), Magnetic fields of the magnetosheath, *Geophys. Rev.*, *14*, 117.

Farrugia, C. J., H. K. Biernat, N. V. Erkaev, L. M. Kistler, G. Le, and C. T. Russell (1998), MHD model of magnetosheath flow: Comparison with AMPTE/IRM observations on 24 October, 1985, *Ann. Geophys.*, *16*, 518.

Frandsen, A. M. A., B. V. Connor, J. V. Van Amersfoort, and E. J. Smith (1978), The ISEE-C vector helium magnetometer, *IEEE Trans. Geosci. Electron.*, *GE-16*, 195.

Hammond, C. M., J. L. Phillips, and A. Balogh (1995), Ulysses observations of slow mode transition in the Jovian magnetosheath, *Eos Trans. AGU*, *76*(17), 5251.

Hubert, D. (2001), Interplanetary magnetic field variations and slow mode transitions in the Earth's magnetosheath, *Geophys. Res. Lett.*, *28*, 1451.

Hubert, D., and C. C. Harvey (2000), Interplanetary rotational discontinuities: From the solar wind to the magnetosphere through the magnetosheath, *Geophys. Res. Lett.*, *27*, 3149.

Hubert, D., C. C. Harvey, M. Roth, and J. De Keyser (1998), Electron density at the subsolar magnetopause for high magnetic shear: ISEE 1 and 2 observations, *J. Geophys. Res.*, *103*, 6685.

Hudson, P. D. (1970), Discontinuities in an anisotropic plasma and their identification in the solar wind, *Planet. Space Sci.*, *18*, 1611.

Lacombe, C., and G. Belmont (1995), Waves in the Earth's magnetosheath: Observations and interpretations, *Adv. Space Res.*, *15*(8/9), 329.

Lee, L. C., M. Yan, and J. G. Hawkins (1991), A study of slow-mode structure in the dayside magnetosheath, *Geophys. Res. Lett.*, *18*, 381.

Lees, L. (1964), Interaction between the the solar plasma wind and the geomagnetic cavity, *AIAA J.*, *2*, 1576.

Luhman, J. G., C. T. Russell, and R. C. Elphic (1986), Spatial distribution of magnetic field fluctuations in the dayside magnetosheath, *J. Geophys. Res.*, *91*, 1711.

Ness, N. F., C. S. Scearce, and J. B. Seek (1964), Initial result of the IMP 1 magnetic field experiment, *J. Geophys. Res.*, *69*, 3531.

Neugebauer, M., D. R. Clay, B. E. Goldstein, B. T. Tsurutani, and R. D. Zwickl (1984), A reexamination of rotational and tangential discontinuities in the solar wind, *J. Geophys. Res.*, *89*, 5395.

Ogilvie, K. W., J. D. Scudder, and H. Doong (1978), The electron spectrometer experiment on ISEE-1, *IEEE Trans. Geosci. Electron.*, *GE-16*, 261.

Paschmann, G., N. Sckopke, G. Haerendel, J. Papamastorakis, S. J. Bame, J. R. Asbridge, J. T. Gosling, E. W. Hones, and E. R. Techh (1978), Plasma observations near the susolar magnetopause, *Space Sci. Rev.*, *22*, 717.

Pudovkin, M. I., M. F. Heyn, and V. V. Lebedeva (1982), Magnetoheath's parameters and their dependence on intensity and direction of the solar wind magnetic field, *J. Geophys. Res.*, *87*, 8131.

Richardson, J. R., and K. I. Paularena (2001), Plasma and magnetic field correlations in the solar wind, *J. Geophys. Res.*, *106*, 239.

Russell, C. T. (1978), The ISEE 1 and 2 fluxgate magnetometers, *IEEE Trans. Geosci. Electron.*, *GE-16*, 239.

Samsonov, A., and D. Hubert (2004), Steady state slow shock inside the Earth's magnetosheath: To be or not to be? 2. Numerical three-dimensional MHD modeling, *J. Geophys. Res*, doi:10.1029/2003JA010008.

Samsonov, A., M. I. Pudowkin, P. Gary, and D. Hubert (2001), Anisotropic MHD model of the dayside magnetosheath downstream of the oblique bow shock, *J. Geophys. Res.*, *106*, 21,689.

Shue, J.-H., J. K. Chao, H. C. Fu, C. T. Russell, P. Song, K. K. Khurana, and H. J. Singer (1997), A new functional form to study the solar wind control of the magnetopause size and shape, *J. Geophys. Res.*, *102*, 9497.

Sibeck, D. G. (1994), Transient and quasi-periodic, (5–15 min) events in the outer magnetosphere, in *Solar Wind Sources of Magnetospheric Ultra-Low Frequency Waves*, *Geophys. Monogr. Ser.*, vol. 81, edited by M. J. Engebretson, K. Takahashi, and M. Scholer, pp. 173–182, AGU, Washington, D. C.

Sibeck, D. G., and J. T. Gosling (1996), Magnetosheath density fluctuations and magnetopause motion, *J. Geophys. Res.*, *101*, 31.

Sibeck, D. G., R. E. Lopez, and E. C. Roelof (1991), Solar wind control of the magnetopause shape, location, and motion, *J. Geophys. Res.*, *96*, 5489.

Siscoe, G. L., L. Davis, P. J. Coleman, E. J. Smith, and D. E. Jones (1968), Power spectra and discontinuities of the interplanetary magnetic field, *J. Geophys. Res.*, *73*, 61.

Song, P., and C. T. Russell (1997), What do we really know about the magnetosheath?, *Adv. Space Res.*, *20*(4/5), 747.

Song, P., and C. T. Russell (2002), Flow in the magnetosheath: The legacy of John Spreiter, *Planet. Space Sci.*, *50*, 447.

Song, P., C. T. Russell, J. T. Gosling, M. Thomsen, and R. C. Elphic (1990), Observations of the density profile in the magnetosheath near the stagnation streamline, *Geophys. Res. Lett.*, *17*, 2035.

Song, P., C. T. Russell, and M. F. Thomsen (1992a), Slow mode transition in the frontside magnetosheath, *J. Geophys. Res.*, *97*, 8295.

Song, P., C. T. Russell, and M. F. Thomsen (1992b), Waves in the inner magnetosheath: A case study, *Geophys. Res. Lett.*, *19*, 2191.

Song, P., C. T. Russell, T. I. Gombosi, J. R. Spreiter, S. S. Stahara, and X. X. Zhang (1999a), On the process in the terrestrial magnetosheath: 1. Scheme development, *J. Geophys. Res.*, *104*, 22,357.

Song, P., C. T. Russell, X. X. Zhang, S. S. Stahara, J. R. Spreiter, and T. I. Gombosi (1999b), On the process in the terrestrial magnetosheath: 2. Case study, *J. Geophys. Res.*, *104*, 22,357.

Sonnerup, B. U. Ö., and L. J. Cahill (1967), Magnetopause structure and attitude from Explorer 12 observations, *J. Geophys. Res.*, *72*, 171.

Southwood, D. J., and M. G. Kivelson (1992), On the form of the flow in the magnetosheath, *J. Geophys. Res.*, *97*, 2873.

Southwood, D. J., and M. G. Kivelson (1995a), The formation of slow mode fronts in the magnetosheath, in *Physics of the Magnetopause*, *Geophys. Monogr. Ser.*, vol. 90, edited by P. Song and B. U. Ö. Sonnerup, pp. 109–119, AGU, Washington, D. C.

Southwood, D. J., and M. G. Kivelson (1995b), Magnetosheath flow near the subsolar magnetopause: Zwan-Wolf and Southwood-Kivelson theories reconciled, *Geophys. Res. Lett.*, *22*, 3275.

Spreiter, J. R., and W. P. Jones (1963), On the effect of a weak interplanetary magnetic field on the interaction between the solar wind and the geomagnetic field, *J. Geophys. Res.*, *68*, 3555.

Spreiter, J. R., A. L. Summers, and A. Y. Alksne (1966), Hydromagnetiv flow around the magnetosphere, *Planet. Space Sci.*, *14*, 223.

Weimer, D. R., D. M. Ober, N. C. Maynard, W. J. Burke, M. R. Collier, D. J. McComas, N. F. Ness, and C. W. Smith (2002), Variable time delays in the propagation of the interplanetary magnetic field, *J. Geophys. Res.*, *107*(A8), doi:10.1029/2001JA009102.

Zhang, X. X., P. Song, S. S. Stahara, J. R. Spreiter, C. T. Russell, and G. Le (1996), Large scale structures in the magnetosheath: Exogenous or endogenous in origin?, *Geophys. Res. Lett.*, *23*, 105.

Zwan, B. J., and R. A. Wolf (1976), Depletion of solar wind plasma near a planetary boundary, *J. Geophys. Res.*, *81*, 1634.

D. Hubert, Laboratoire d'Etude Spatiale et d'Instrumentation Astrophysique (UMR 8109/CNRS), Observatoire de Paris, 92195 Meudon CEDEX, France. (daniel.hubert@obspm.fr)

A. Samsonov, Department of Earth Physics, Institute of Physics, St. Petersburg State University, St. Petersburg, 198504, Russia.